NOTES AND CORRESPONDENCE

On the Reemergence of North Atlantic SST Anomalies

MICHAEL S. TIMLIN AND MICHAEL A. ALEXANDER

National Oceanic and Atmospheric Administration–Cooperative Institute for Research in Environmental Sciences Climate Diagnostics Center, Boulder, Colorado

CLARA DESER

National Center for Atmospheric Research, Boulder, Colorado*

14 November 2001 and 3 April 2002

ABSTRACT

The reemergence mechanism, whereby temperature anomalies extending over the deep winter mixed layer are stored beneath the surface in summer and are reentrained into the mixed layer when it deepens again in the following autumn and winter, is studied in the North Atlantic using approximately 40 years of surface and subsurface data. Reemergence is found to be robust in the Sargasso Sea and the northeast Atlantic, regions where (i) the mixed layer is much deeper in winter than in summer, (ii) currents are relatively weak, and (iii) temperature anomalies are coherent over broad areas. The two leading empirical orthogonal functions of North Atlantic SST anomalies also exhibit strong reemergence signatures. A novel application of empirical orthogonal function analysis to temperature anomalies in the time–depth plane, which also incorporates information from all grid points, is shown to be an efficient and useful approach for detecting reemergence without dependence on specific spatial patterns or prior selection of regions.

1. Introduction

The upper ocean generally consists of a well-mixed surface layer atop the pycnocline, in which density increases with depth. In midlatitudes, the seasonal evolution of the mixed layer and pycnocline can influence the behavior of temperature anomalies. Temperature anomalies that form over the deep mixed layer in winter are sequestered in the summer seasonal pycnocline when the mixed layer shoals in spring. The anomalies within the statically stable pycnocline are preserved through summer while temperatures in the thin mixed layer are altered by surface fluxes, gradually losing their relationship with those in the previous winter. In autumn, the mixed layer deepens by entraining water from below. As a consequence, a portion of the thermal anomalies created in the previous winter is returned to the surface in the following autumn and winter.

The tendency for sea surface temperature (SST) anomalies to recur from one winter to the next without persisting through the intervening summer was first noted by Namias and Born (1970, 1974). Based on subsurface data collected at ocean weather ships and mixed layer model simulations, Alexander and Deser (1995) documented that the wintertime mixed layer thermal anomalies, stored in the summer pycnocline, did reemerge at the surface in the following autumn/winter. Alexander et al. (1999, 2001) showed that this ''reemergence mechanism'' occurs in several regions of the North Pacific and across much of the basin. The latter was suggested by the evolution of the leading pattern of SST variability over the seasonal cycle and by the strong relationship between the dominant pattern of temperature anomalies at the surface in March and November with the pattern beneath the mixed layer in September.

The aforementioned studies primarily focused on reemergence in the North Pacific Ocean. Bhatt et al. (1998) and Watanabe and Kimoto (2000, hereinafter WK) analyzed the seasonal evolution of temperature anomalies in the North Atlantic based on the leading empirical orthogonal function (EOF) of air temperature, in the case of Bhatt et al., and SST, in the case of WK. The first EOF of air temperature from the one study and

* The National Center for Atmospheric Research is sponsored by the National Science Foundation.

Corresponding author address: Michael S. Timlin, Dept. of Atmospheric Sciences, University of Illinois at Urbana–Champaign, 105 S. Gregory St., Urbana, IL 61801.
E-mail: timlin@cdc.noaa.gov

that of SST from the other study in winter are largely similar, with one center in the northeast Atlantic and another off the east coast of the United States (the latter is ~5° of latitude farther south in Bhatt et al. as compared with WK). Watanabe and Kimoto (2000) found evidence for reemergence in their two midlatitude regions; Bhatt et al., studying similar areas, detected reemergence only in their northernmost one. Differences in period of record and regional boundaries may have contributed to the different findings in the two studies. For example, the EOF analyses in WK extended farther south and included a third center of variability located to the east of Africa between 10° and 25°N. However, reemergence did not occur there, because the annual cycle in mixed layer depth is small in the subtropics.

The aim of this study is to expand upon the findings of WK by examining the evolution of upper-ocean temperature anomalies in the North Atlantic from both a regional and basinwide perspective. We employ traditional lag correlation analysis, EOF analysis in the time–depth plane for selected regions, EOF analysis of basinwide SST anomalies, and a new EOF approach in which basinwide temperature anomaly fields are analyzed in the time–depth plane.

2. Data

Our analyses are performed on monthly fields from two independent ocean temperature datasets. SSTs were obtained from version 2.3b of the Global Sea Ice and Sea Surface Temperature (GISST; Rayner et al. 1996) dataset. The fields are on a 1° × 1° latitude–longitude grid for the period of 1958–97. Subsurface data from the Joint Environmental Data Analysis Center (JEDAC) contain temperatures at 11 levels (0, 20, 40, 60, 80, 120, 160, 200, 240, 300, and 400 m) during 1955–95. Optimal interpolation was used in the JEDAC analyses to generate temperature values on a 2° × 5° grid based on measurements from bathythermographs and Nansen casts (White 1995). Although there are approximately an order of magnitude fewer upper-ocean temperature profiles than SST observations, a detailed examination of the JEDAC fields indicated that the number of profiles in the North Atlantic is sufficient to resolve the reemergence mechanism.

Prior to our computations, the GISST and JEDAC data were interpolated to the same 5° × 5° grid. All analyses were performed on monthly temperature anomalies that were obtained by removing the long-term monthly means from the original data.

Differences in the mean mixed layer depth between winter and summer are used to identify regions in which reemergence is likely to occur. The climatological mixed layer depths, obtained from the *World Ocean Atlas 1994* (Monterey and Levitus 1997), are based on density criteria that take both temperature and salinity into account.

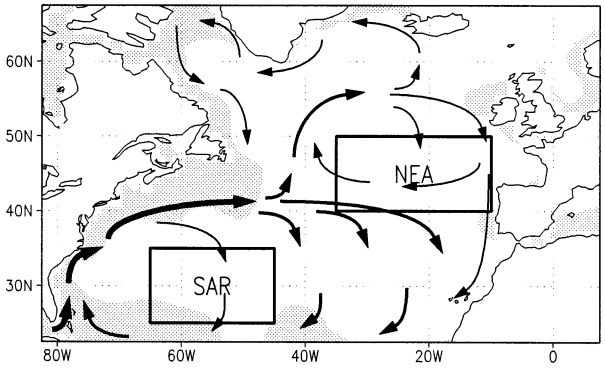

FIG. 1. Map of the North Atlantic region showing currents, mixed layer depth difference threshold, and regions of study. Currents are shown schematically by the arrows; thicker arrows indicate stronger currents. Shading appears in those areas in which the seasonal difference in mixed layer depth (Feb minus Sep) is less than 50 m. The two regions in this study are the SAR region (25°–35°N, 65°–45°W) and the NEA region (40°–50°N, 35°–10°W).

3. Results

a. Regional analyses

We use several factors to select regions in which wintertime SST anomalies are likely to recur. First, the reemergence process requires that the mixed layer is considerably deeper in winter than in summer. Second, reemergence is less likely to occur in the vicinity of strong currents, because the temperature anomalies could be advected away from a region over the course of the seasonal cycle. Eddies associated with currents, such as meanders in the Gulf Stream, could also diffuse temperature anomalies that would otherwise undergo the reemergence process. Third, detection of reemergence is favored in regions in which SST anomalies are spatially coherent. Two regions, the Sargasso Sea (SAR) and the northeast Atlantic (NEA), were selected by considering winter minus summer mixed layer depth, current speed, and the coherence of the temperature anomalies. These regions, along with a schematic depiction of the surface currents in the North Atlantic and areas in which the February minus September mixed layer depth exceeds 50 m, are shown in Fig. 1.

Monthly temperature anomalies from JEDAC were averaged over the SAR and NEA regions at each depth and then were correlated with the temperature anomaly at a ''base point.'' Following Alexander and Deser (1995), we chose a base point (60–80 m in June–July) in the summer pycnocline because it is the link between the descending and return branches of the reemergence process. Correlations between the base-point time series and temperature anomalies between the surface and 160 m from the previous January to the following March are shown for the SAR and NEA regions in Fig. 2. Evidence for the reemergence process is seen in both regions where relatively high correlations extend to the surface in the preceding winter/spring, extend throughout the pycnocline but not the mixed layer during sum-

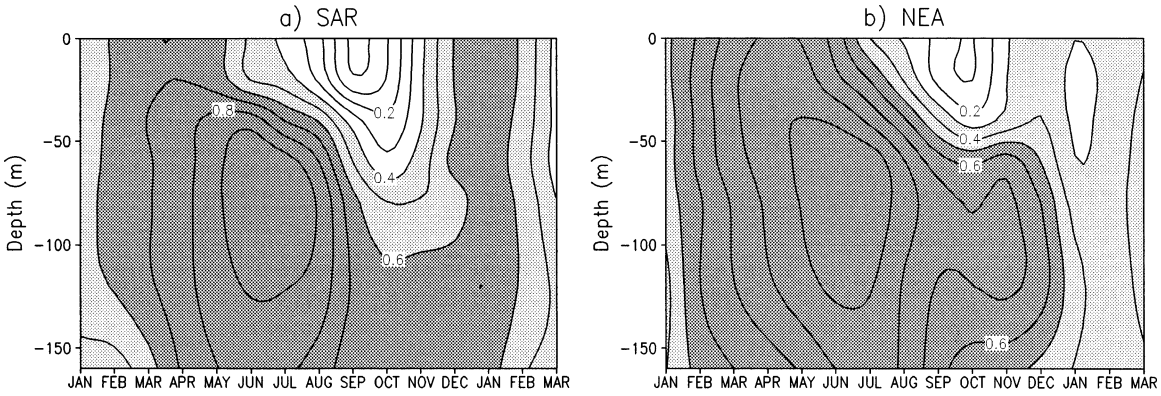

FIG. 2. Lead–lag correlations for (a) SAR and (b) NEA relative to a base-point time series constructed by averaging temperature anomalies for Jun and Jul at 60–80 m depth. Correlations are from the preceding Jan to the following Mar and from the surface to 160 m. Computations are based on 1955–95. The contour interval is 0.1. Light (dark) shading indicates correlation values greater than 0.4 (0.6) in SAR and greater than 0.3 (0.5) in NEA.

mer, and extend back to the surface in the following autumn/winter. Reemergence is very strong in the SAR region, for which the correlations exceed 0.6 through the mixed layer in the previous February–May and the following December–January. In contrast, the correlation structure is asymmetric in the NEA region, with higher correlations in the previous spring than in the following autumn, which suggests that the descending branch of the reemergence process is stronger than the return branch. Oceanic processes such as subduction and diffusion and surface fluxes in autumn that are uncorrelated with those in the previous winter can dilute the thermal anomalies that are returning to the surface. In particular, the NEA region is located primarily within an area of mean negative subduction (Marshall et al. 1993) such that net entrainment of fluid from the main thermocline into the winter mixed layer and summer pycnocline may act to dilute the local atmospherically forced reemergence signal.

To eliminate the subjective choice of a base point, we applied EOF analysis to the regional temperature anomalies as a function of time and depth. The most common EOFs in geophysical research are constructed such that each latitude–longitude grid point is a variable and each time step (monthly value, annual value, or a particular monthly value, e.g., May, from each year) serves as an observation of that variable (Wilks 1995). For reemergence, the pattern of interest is best displayed in a time–depth plane (see Fig. 2), in which time is in months over approximately a year. In according with that, the grid of seven levels (0–160 m) and 15 months (January–March of the following year) serve as the variables, with each year (1955–95) as an observation for our regional EOFs. The principal component (PC) for each EOF is the projection of the original temperature anomalies onto the EOF at each observation, each 15-month period in this case. Hereinafter EOFs will be shown as the correlation between the PC and the monthly temperature anomalies.

The results of the EOF analyses (Fig. 3) are very similar to the lead–lag correlations (Fig. 2) and highlight the reemergence signal. The first EOF explains nearly 50% of the variance in the time–depth plane in both regions. Differences between the lead–lag correlation pattern and the leading EOF pattern in each region are of the same order as differences due to small variations in the base point in the lead–lag correlation analyses. The PC, also shown in Fig. 3, measures the correspondence between the EOF pattern and the temperature anomaly pattern for a given year. The sign of the PC indicates whether the anomaly pattern that year was positive or negative, and the absolute value of the PC indicates the strength of the relationship. The rms value of the PC in the NEA region is greater during the first half of the record than during the second half (2.3 and 1.5, respectively), which suggests that the reemergence mechanism was more vigorous prior to 1975. A comparison of lead–lag correlations in the NEA region for 1955–75 with those in 1975–95 (Timlin et al. 1999) also indicates that reemergence was stronger in the earlier period.

b. Basinwide surface analysis

Is reemergence of basinwide extent in the North Atlantic as it is in the North Pacific? One approach to examine this question is to use a traditional EOF analysis of SST anomalies whose variables are the latitude–longitude grid points in the North Atlantic. Watanable and Kimoto calculated the leading EOF in the North Atlantic in winter and then examined the lead–lag correlations between the associated PC and the projection of monthly SST anomalies in the North Atlantic on the winter EOF pattern. The correlations decreased from near 1.0 in January to ~0.1 in August and then increased to ~0.4 in the following January.

We expand on the WK analysis by computing lag autocorrelations of the leading PC based on SST anom-

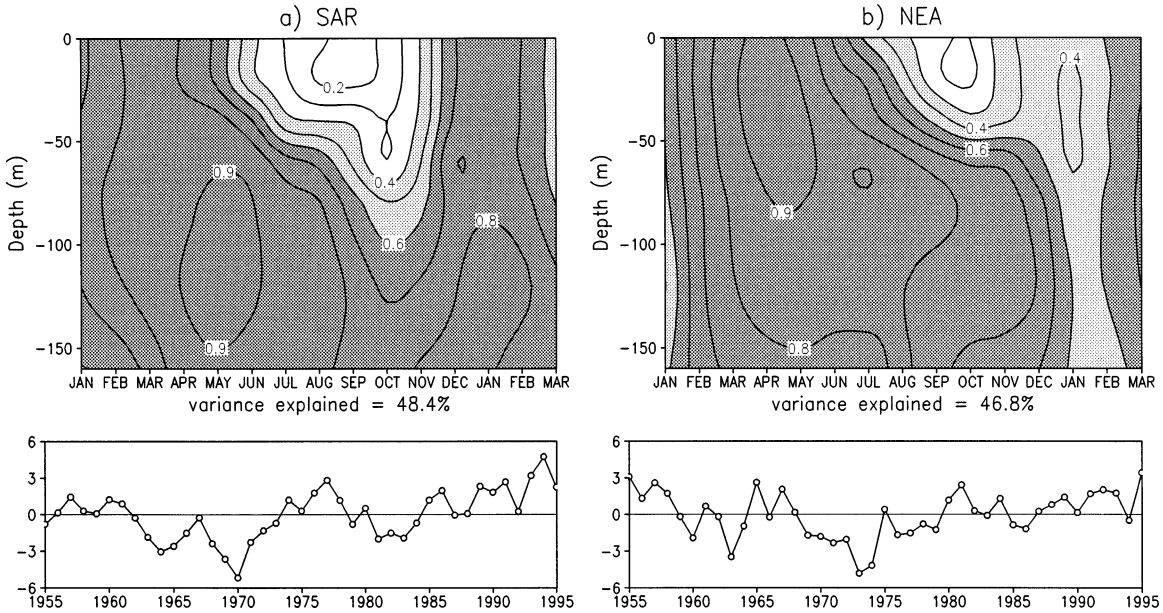

FIG. 3. (top) Time–depth EOF patterns and (bottom) associated PCs for the (a) SAR and (b) NEA regions. The domain of the EOF is from the preceding Jan to the following Mar and from the surface to 160 m. The EOF pattern is shown as the correlation between the PC record and the temperature anomaly time series. Computations are based on 1955–95. Contour interval is 0.1. Shading is as in Fig. 2.

alies in all months from 1955 to 1998. Prior to the EOF analysis, the standard deviation of Atlantic SST anomalies averaged over 20°–70°N is computed for each month (ranging from 0.46 in February to 0.60 in July), and then the anomalies at each grid point are scaled by the basinwide standard deviation from the corresponding month to deemphasize the seasonal cycle in the variability while retaining the variability from one location to another. The first EOF and PC are shown in Fig. 4. The leading pattern is similar to EOF analyses of North Atlantic SST anomalies obtained in previous studies (e.g., Wallace et al. 1993; Cayan 1992; Deser and Blackmon 1993; WK). Figure 5 shows the correlations of the leading PC calculated separately for each calendar month (vertical axis) with the PC in subsequent months from lag 0 to lag +12 (horizontal axis). A similar analysis was shown in Kushnir et al. (2002). The correlations decrease over lags of 3 months regardless of the initial month, with especially strong decay starting from September when the mixed layer is shallowest. This result is consistent with the stochastic theory for SST variability (e.g., Frankignoul and Hasselmann 1977), which indicates that SST anomalies driven by random surface forcing decay exponentially because of damping of SST anomalies by air–sea heat fluxes at a rate that is inversely proportional to mixed layer depth. In Fig. 5, however, correlations lagged from winter months first decrease but then rise as the lag increases; for example, correlations based on the PC value in March rise from less than 0.3 at a lag of 5 months (August) to greater than 0.7 at a lag of 10 months (January). Consistent with the reemergence hypothesis, the increases at longer lags are not apparent in correlations with late summer values. Figure 5 does suggest that SST anomalies as late as June and July recur 5–6 months later. Analysis of the second PC (not shown) also contains the reemergence signal, although it is weaker than

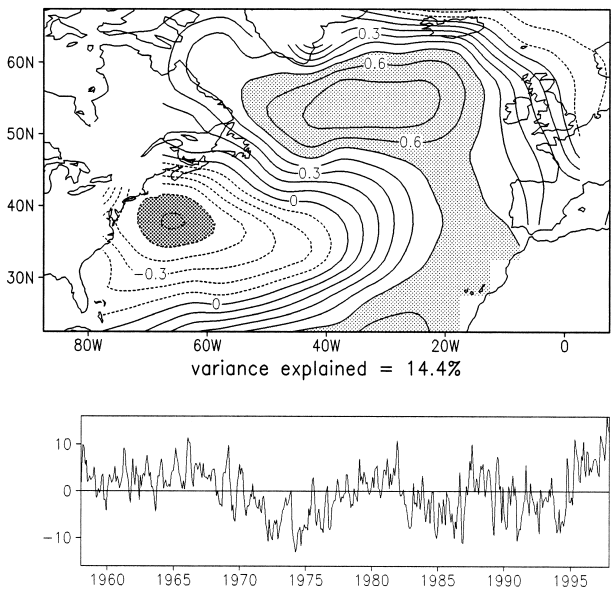

FIG. 4. Leading EOF of monthly SST anomalies and the associated PC time series based upon 1958–97. The data in each calendar month are scaled by their spatial standard deviation so that the PC is equally weighted through the seasonal cycle. The EOF pattern is shown as the correlation between the PC record and the temperature anomaly time series at each grid point. The contour interval is 0.1. Light (dark) shading indicates values >0.5 (<-0.5).

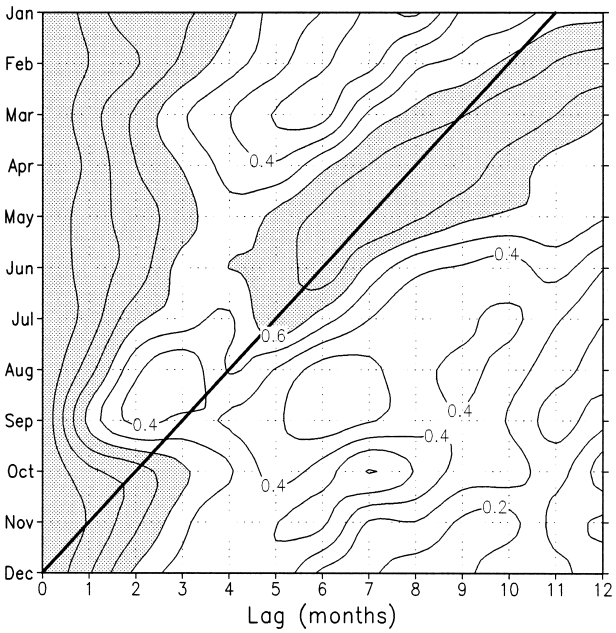

FIG. 5. Lagged correlations of the PC time series from Fig. 4 calculated separately for each calendar month to show seasonal differences in evolution. The contour interval is 0.1. Shading indicates correlations exceeding 0.6. The black diagonal line is a visual aid locating Dec.

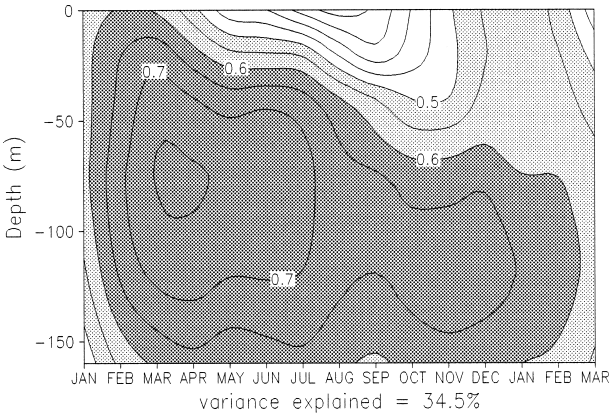

FIG. 6. Pattern of the basinwide time–depth EOF shown as the correlation between the associated PC (not shown) and the temperature anomalies for each month and depth. See text for further explanation. The contour interval is 0.05. Light (dark) shading indicates correlations exceeding 0.5 (0.6).

in the leading PC. Thus, the reemergence signal is not necessarily tied to a particular SST pattern, because it appears in both of the leading PCs and because it is readily apparent in regions that are not located in the centers of the leading EOF (cf. Figs. 1–3 with Fig. 4a).

c. Basinwide depth-dependent analysis

Here we present a new approach for tracking reemergence over the North Atlantic by performing EOF analysis in the time–depth plane (similar to the regional EOFs) but incorporating information from all grid points over the domain. To accomplish this, we allow each 5° × 5° grid point in each year to represent a separate observation of the time–depth plane for the EOF analysis. We tested this method on the North Pacific data, and the results compared favorably with those reported in Alexander et al. (1999). For the North Atlantic, the variables used to compute the EOF are seven depths (from 0 to 160 m) and 15 months from January to March of the following year. The PC consists of 4879 observations: 119 (the number of 5° × 5° grid points in the analysis domain) × 41 (the number of years). The leading EOF, which explains 34.5% of the variance, is shown in Fig. 6. It accounts for less variance than its regional counterparts (SAR 48.4%, NEA 46.8%) because of local variations in the timing and vertical structure of the reemergence process and by including some areas in which reemergence does not occur. The reemergence pattern seen in earlier time–depth plots is again evident here: high correlations through the mixed layer of the first winter, low (high) correlations at (below) the surface layer in summer, and then rising correlations at the surface through autumn and into the following winter. Surface correlations can be seen to decay quickly from February (>0.6) through August (<0.3) when the mixed layer is shoaling, and then to rebound from August to December (>0.5) as water from the summer pycnocline is reentrained into the deepening mixed layer.

4. Summary and discussion

A variety of approaches have been used to examine the seasonal evolution of upper-ocean temperature anomalies in the North Atlantic during 1955–95. A regional approach based on three selection criteria identified two areas in which reemergence was expected to occur: the Sargasso Sea and the northeast Atlantic. The results, based on traditional lead–lag correlation analysis from a subsurface base point in summer and from EOF analysis in the time–depth plane, confirm strong reemergence in the Sargasso Sea region (correlations in the mixed layer that exceed 0.6 from the previous February–May to the following December–January) and somewhat weaker reemergence in the northeast Atlantic region. Reemergence in the latter region was shown to be more vigorous prior to 1975 than after. A basinwide surface analysis showed that the leading EOF of monthly SST anomalies in the North Atlantic, a north–south dipole pattern, exhibits strong reemergence, in agreement with previous studies (Bhatt et al. 1998; WK). We note, however, that the second EOF also exhibits reemergence and that the SAR and NEA regions are not at the centers of action of either of the two leading EOF patterns, indicating that reemergence is not constrained to any particular spatial pattern. Last, a novel application of EOF analysis to temperature anomalies in the time–depth plane, but one that also incorporates information

from all grid points over the domain, was shown to be a useful approach for detecting reemergence without being dependent upon any particular spatial pattern or prior selection of regions.

Acknowledgments. We thank Warren White and Ted Walker for providing the JEDAC data and the CDC data group for providing the GISST and WOA94 data. We benefitted greatly from discussions with Yochanan Kushnir regarding the SST EOF analysis. The suggestions by the anonymous reviewers were helpful and were much appreciated. Graphics were generated using GrADS software developed at COLA. This work was supported in part by a grant from the NOAA OGP Clivar Program and by an omnibus grant from NOAA OGP to CDC.

REFERENCES

Alexander, M. A., and C. Deser, 1995: A mechanism for the recurrence of wintertime midlatitude SST anomalies. *J. Phys. Oceanogr.,* **25,** 122–137.

——, ——, and M. S. Timlin, 1999: The reemergence of SST anomalies in the North Pacific Ocean. *J. Climate,* **12,** 2419–2433.

——, M. S. Timlin, and J. D. Scott, 2001: Winter-to-winter recurrence of sea surface temperature, salinity and mixed layer depth anomalies. *Progress in Oceanography,* Vol. 49, Pergamon, 41–61.

Bhatt, U. S., M. A. Alexander, D. S. Battisti, D. D. Houghton, and L. M. Keller, 1998: Atmosphere–ocean interaction in the North Atlantic: Near-surface climate variability. *J. Climate,* **11,** 1615–1632.

Cayan, D. R., 1992: Latent and sensible heat flux anomalies over the northern oceans: Driving the sea surface temperature. *J. Phys. Oceanogr.,* **22,** 859–881.

Deser, C., and M. L. Blackmon, 1993: Surface climate variations over the North Atlantic Ocean during winter: 1900–1989. *J. Climate,* **6,** 1743–1753.

Frankignoul, C., and K. Hasselmann, 1977: Stochastic climate models. Part 2. Application to sea-surface temperature variability and thermocline variability. *Tellus,* **29,** 284–305.

Kushnir, Y., W. A. Robinson, I. Bladé, N. M. J. Hall, S. Peng, and R. Sutton, 2002: Atmospheric GCM response to extratropical SST anomalies: Synthesis and evaluation. *J. Climate,* **15,** 2233–2256.

Marshall, J. C., A. J. G. Nurser, and R. G. Williams, 1993: Inferring the subduction rate and period over the North Atlantic. *J. Phys. Oceanogr.,* **23,** 1315–1329.

Monterey, G., and S. Levitus, 1997: *Seasonal Variability of Mixed Layer Depth for the World Ocean.* NOAA Atlas NESDIS 14, 96 pp.

Namias, J., and R. M. Born, 1970: Temporal coherence in North Pacific sea-surface temperature patterns. *J. Geophys. Res.,* **75,** 5952–5955.

——, and ——, 1974: Further studies of temporal coherence in North Pacific sea surface temperatures. *J. Geophys. Res.,* **79,** 797–798.

Rayner, N. A., E. B. Horton, D. E. Parker, C. K. Folland, and R. B. Hackett, 1996: Version 2.2 of the Global Sea-Ice and Sea Surface Temperature data set 1903–1994. Climate Research Tech. Note 74, 35 pp. [Available from Hadley Centre for Climate Prediction and Research, London Rd., Bracknell, Berkshire RG12 2SY, United Kingdom.]

Timlin, M. S., M. A. Alexander, and C. Deser, 1999: Re-emergence of SST anomalies in the North Atlantic Ocean. Preprints, *Eighth Conf. on Climate Variations,* Denver, CO, Amer. Meteor. Soc., 126–128.

Wallace, J. M., Y. Zhang, and K.-H. Lau, 1993: Structure and seasonality of interannual and interdecadal variability of the geopotential height and temperature fields in the Northern Hemisphere troposphere. *J. Climate,* **6,** 2063–2082.

Watanabe, M., and M. Kimoto, 2000: On the persistence of decadal SST anomalies in the North Atlantic. *J. Climate,* **13,** 3017–3028.

White, W. B., 1995: Design of a global observing system for gyre-scale upper ocean temperature variability. *Progress in Oceanography,* Vol. 36, Pergamon, 169–217.

Wilks, D. S., 1995: *Statistical Methods in the Atmospheric Sciences.* Academic Press, 464 pp.